Chemical forms of selenium in the metal-resistant bacterium Ralstonia metallidurans CH34 exposed to selenite and selenate

Geraldine Sarret, Laure Avoscan, Marie Carrière, Richard Collins, Nicolas Geoffroy, Francine Carrot, Jacques Covès, Barbara Gouget

▶ **To cite this version:**

Geraldine Sarret, Laure Avoscan, Marie Carrière, Richard Collins, Nicolas Geoffroy, et al.. Chemical forms of selenium in the metal-resistant bacterium Ralstonia metallidurans CH34 exposed to selenite and selenate. Journal of Gambling Studies, 2005, 71, pp.2331-2337. hal-00022629

HAL Id: hal-00022629
https://hal.science/hal-00022629

Submitted on 12 Apr 2006

HAL is a multi-disciplinary open access archive for the deposit and dissemination of scientific research documents, whether they are published or not. The documents may come from teaching and research institutions in France or abroad, or from public or private research centers.

L'archive ouverte pluridisciplinaire **HAL**, est destinée au dépôt et à la diffusion de documents scientifiques de niveau recherche, publiés ou non, émanant des établissements d'enseignement et de recherche français ou étrangers, des laboratoires publics ou privés.

Chemical forms of selenium in the metal-resistant bacterium *Ralstonia metallidurans* CH34 exposed to selenite and selenate

Running title: Chemical forms of Se in *Ralstonia metallidurans* CH34

Géraldine Sarret [1*], Laure Avoscan [2], Marie Carrière [2], Richard Collins [2], Nicolas Geoffroy [1], Francine Carrot [2], Jacques Covès [3], and Barbara Gouget [2]

[1] Environmental Geochemistry Group, LGIT, University of Grenoble and CNRS, BP 53, 38041 Grenoble, Cedex 9, France.

[2] Laboratoire Pierre Süe, CEA-CNRS UMR 9956, CEA/Saclay, 91191 Gif-sur-Yvette, France.

[3] Institut de Biologie Structurale - J.-P. Ebel, Laboratoire des Protéines Membranaires, 41 rue Jules Horowitz, 38027 Grenoble Cedex, France.

*Corresponding author: Environmental Geochemistry Group, LGIT, University of Grenoble and CNRS, BP 53, 38041 Grenoble, Cedex 9, France. Tel +33 (0)4 76 82 80 21; Fax: +33 (0)4 76 82 81 01, email: gsarret@ujf-grenoble.fr.

Abstract

Ralstonia metallidurans CH34, a soil bacterium resistant to a variety of metals, is known to reduce selenite to intracellular granules of elemental selenium (Se^0). We have studied the kinetics of selenite (Se^{IV}) and selenate (Se^{VI}) accumulation and used X-ray absorption spectroscopy to identify the accumulated form of selenate, as well as possible chemical intermediates during the transformation of these two oxyanions. When introduced during the lag phase, the presence of selenite increased the duration of this phase, as previously observed. Selenite introduction was followed by a period of slow uptake, during which the bacteria contained Se^0 and alkyl selenide in equivalent proportions. This suggests that two reactions with similar kinetics take place: an assimilatory pathway leading to alkyl selenide, and a slow detoxification pathway leading to Se^0. Subsequently, selenite uptake strongly increased (up to 340 mg Se per g of proteins), and Se^0 was the predominant transformation product, suggesting an activation of selenite transport and reduction systems after several hours of contact. Exposure to selenate did not induce an increase in the lag phase duration and the bacteria accumulated approximately 25 fold less Se than when exposed to selenite. Se^{IV} was detected as transient species in the first 12 hours after selenate introduction, Se^0 also occurred as minor species, and the major accumulated form was alkyl selenide. Thus, in the present experimental conditions selenate mostly follows an assimilatory pathway, and the reduction pathway is not activated upon selenate exposure. These results show that *R. metallidurans* CH34 may be suitable for the remediation of selenite - but not selenate - contaminated environments.

Introduction

Microorganisms play a major role in the biogeochemical cycle of selenium in the environment (12). Certain strains that are resistant to selenium oxyanions, and reduce selenite (Se^{IV}) and/or selenate (Se^{VI}) to the less available elemental selenium (Se^{0}) (7), could be potentially used for the bioremediation of contaminated soils, sediments, industrial effluents and agricultural drainage waters.

Ralstonia metallidurans CH34 is a soil bacterium characteristic of metal-contaminated biotopes. It is resistant to a variety of heavy metals and metalloids including Cr^{VI}, Co^{II}, Ni^{II}, Cu^{II}, Zn^{II}, As^{V}, Cd^{II}, Hg^{II}, and Pb^{II}. The genes for metal resistance are located in two large plasmids (pMOL28 and pMOL30). Their function and regulation are well understood for some of these elements (18). This bacterial strain is also resistant to selenite and detoxification is realized by the incorporation of this oxyanion and its subsequent reduction to red Se^{0}, as shown by X-ray absorption spectroscopy (XAS) (24). This study also revealed that the Se^{0} granules were mainly localized in the cytoplasm. In contrast to previously cited metals and metalloids, the genes involved in selenite resistance have not been yet identified, and the exact mechanism of selenite bioreduction is still unknown. *R. metallidurans* CH34 can also resist up to 16 mM selenate (2). The capacity of *R. metallidurans* CH34 to accumulate selenate, and the fate of this oxyanion following incorporation have never been investigated. We have now studied the kinetics of selenite and selenate accumulation, and used X-ray absorption near-edge structure (XANES) spectroscopy to determine Se speciation in order to identify the chemical intermediates putatively appearing during reduction. For such a purpose, XANES is the method of choice since it is non-destructive and enables direct determination of the target element speciation, *i.e.*, its oxidation state and sometimes its exact chemical form. The results obtained on speciation were combined with the total metal content of each sample in order to deduce the concentration of each metal species. Such quantitative information is particularly useful to estimate the relative importance of several chemical pathways in a particular system.

Materials and Methods

Bacterial strain and growth media. *R. metallidurans* CH34 provided by Prof. Max Mergeay (SCK/CEN, Mol, Belgium) was grown aerobically at 29°C in Tris salt mineral medium (TSM) with 2% gluconate as a carbon source (18, 19) .

One-contaminant (Se^{IV} or Se^{VI}) exposure. A preculture was obtained by growing the cells until mid-exponential phase (absorbance at 600 nm, A_{600} = 1.5). Cells were then appropriately

diluted to inoculate 300 ml TSM at an initial A_{600} of 0.3. The cultures were monitored by recording the A_{600} as a function of time. A first series of experiment was run by adding selenite or selenate at a final concentration of 2 mM at zero time (A_{600} = 0.3). In a second set of experiments, the selenium oxyanion was added during the first half of the exponential phase (A_{600} = 1). Finally, a third series was run by adding the selenium oxyanion at the beginning of the stationary phase (A_{600} = 3). Sodium selenite and sodium selenate were prepared as 1 M stock solution in ultra-pure water and sterilized by filtration. Control cultures were grown under identical conditions in the absence of the selenium oxyanions. 5 to 15 mL depending on the turbidity of the cell suspension were sampled at various time intervals during 6 days, centrifuged and the pellets were freeze-dried and stored for further use. Cell yield was determined by recording the A_{600} and assaying the protein content (BCA method with bovine serum albumin as standard).

Two-contaminant (Se^{IV} and Se^{VI}) exposure. Cultures of *R. metallidurans* CH34 were inoculated to an absorbance at 600 nm of 3 (stationary phase) and exposed to two different mixtures of selenite and selenate (2 mM selenite and 2 mM selenate, or 1 mM selenite and 10 mM selenate). Three cases were tested: i) selenite and selenate were both added immediately after inoculation, ii) selenite was added immediately after inoculation and selenate 3h later, iii) selenate was introduced immediately after inoculation and selenite 3h later. A control culture, under identical conditions, was grown in the presence of selenite alone added immediately after inoculation. The appearance of the red color, sign of the reduction of selenite to Se^0, was checked after 24h of exposure.

ICP-MS analyses. Bacteria and culture medium were separated by centrifugation at 6000 g for 10 min. Cell pellets were washed twice with ultra-pure water at 4°C and re-suspended in a minimum volume of ultra-pure water. A fraction of the pellet was digested in a mixture of NaOH 1 M / SDS 20%. In order to fully solubilise elemental selenium, H_2O_2 was added to the digested sample until the characteristic red color disappeared. These samples were used to determine total Se accumulation.

Selenium concentrations were measured by inductively coupled plasma - mass spectrometry (ICP-MS) using an X7 Series quadrupole instrument (Thermo Electron Corporation, Cergy-Pontoise, France). Calibration curves were obtained by analysis of a range of SPEX certiPrep selenium standards (Metuchen, NJ, USA). Selenium concentrations were determined with the isotopes 79 and 82 and yttrium was used as an internal standard (1 $\mu g\ l^{-1}$). For digested bacteria analyses, samples were acidified with ultra-pure 65% nitric acid

(Normatom quality grade, Prolabo, Fontenay sous Bois, France) and diluted in ultra-pure water.

X-ray absorption spectroscopy. Selenium K-edge X-ray absorption experiment were performed on beamline FAME (BM30B) of the European Synchrotron Radiation Facility. The Se model compounds (all in solid state unless noted) used for this study were the following: hexagonal (gray) elemental selenium, sodium selenate (solid and in solution), sodium selenite (solid and in solution), selenium sulfide, selenium dioxide, dimethyl selenide in solution, selenomethionine, S-methyl seleno L-cysteine, seleno-DL-cystine, seleno-cystamine, selenodiglutathione in solution, selenourea, and selenoguanosine. Selenodiglutathione was prepared by mixing sodium selenite and GSH with a molar ratio 1:4 in a dilute HCl solution (pH 1.3) (10). A bacterial pellet of *R. metallidurans* CH34 exposed to selenite during 10 days, and which was shown to contain monoclinic (red) Se^0 (24), was used as a reference for this compound. The other compounds were purchased from Sigma-Aldrich. Freeze-dried bacteria were ground in an agate mortar and diluted with glucose when necessary. The mixture was pressed into 5-mm-diameter pellets prior to XANES measurements.

The spectra were recorded at room temperature in fluorescence mode using a 30-element solid-state Ge detector (Canberra) for the most diluted bacterial samples and in transmission mode, using a diode, for the more concentrated samples. The monochromator was a Si(220) double crystal. Two to four scans of 10 min were summed, depending on Se concentration. The position of the beam on the pellet was changed between each scan in order to limit radiation damage. Hexagonal Se(0) was recorded simultaneously, and the spectra were energy calibrated by setting the energy of the maximum of the white line for this reference spectrum at 12.6592 keV. XANES spectra were normalized using polynomial functions of degree 1 and 3 for the pre-and post-edge parts, respectively. Each set of spectra for a given kinetics experiment was treated by principal component analysis (PCA) (17, 30). This approach allows the determination of the number of Se species present in a set of samples, and to identify these species, using a library of reference spectra. The number of principal components was determined based on the eigenvalue of each component, and on the quality of the reconstructed spectra using 1, 2, 3, or more components using the total normalized sum-squares residual (*Total NSS*):

$$Total\ NSS = \sum_{spectra} \sum_{i} \left[\mu_{exp.} - \mu_{reconst.}\right]^2 / \sum_{spectra} \sum_{i} \left[\mu_{exp.}\right]^2 \cdot 100 \qquad (1)$$

where μ is the normalized absorbance. The principal components were identified by target transformation using the *NSS* criterion.

$$NSS = \sum_i \left[\mu_{exp.} - \mu_{reconst.}\right]^2 / \sum_i \left[\mu_{exp.}\right]^2 \cdot 100 \qquad (2)$$

The percentage of each species, in molar fraction of Se, was then determined by linear combination fitting (LCF) of each spectrum using the spectra of the identified reference materials. The precision is estimated at ± 5 % of total Se. The percentages were then multiplied by total Se content, as determined by ICP-MS, in order to obtain the concentrations of each species (mg of Se per g of proteins).

Results

The sensitivity of Se K-edge XANES spectroscopy for probing the oxidation state of Se is well established (20, 21). Figure 1 displays some of the reference spectra used in this study. The main peak of Se^{IV} and Se^{VI} is shifted by + 4.5 eV and + 7.5 eV, respectively, relative to Se^0. The energy shift is much smaller for organoselenium compounds (+ 0.4 to + 1.5 eV relative to Se^0, depending on the type of compound). The position of the main peak is identical for compounds with similar Se environments, for instance S-methyl selenocysteine and selenomethionine for alkyl selenide (RSeR), seleno-DL cystine and selenocystamine for alkyl diselenide (RSeSeR), and selenourea and selenoguanosine for Se-C double bond (not shown). The energy shift between two types of Se local structures, for instance RSeSeR and RSSeSR, can be as small as 0.5 eV. The sensitivity of XANES is probably not sufficient to determine the distribution of several types of organic Se in a complex mixture, but it certainly enables the identification of the major organoselenium species.

Selenite exposure

In a first experiment, a culture of *R. metallidurans* CH34 was exposed to 2 mM selenite added at the beginning of growth (A_{600} = 0.3). As described previously (24), the presence of selenite induced an increase in the lag phase duration (approximately 48h compared to 10h in the absence of selenite). The accumulation of selenite was minimal during this phase (< 40 mg Se per g of proteins). However, at the end of the exponential phase, and during the stationary phase, selenium was strongly accumulated: at t = 144h, Se accounted for one third of the protein weight (Fig. 2).

Selected XANES spectra for the bacteria at various exposure times are shown in Figure 3. The position of the main peak for t = 0h at 12.6637 keV and the presence of a shoulder on

the left-hand part of the peak suggest that the bacteria contain selenite and a minor proportion of organoselenium. At higher exposure times (t = 1h to 48h), the spectra are identical, and the maximum of the main peak is intermediate between RSeR and Se^0 (12.6599 keV). The main peak is then slightly shifted to the left at t = 96h (12.6596 keV), and matches the position of Se^0 at t = 120 and 144h (12.6592 keV). PCA showed that this set of spectra could be described by three components (eigenvalues 80.0, 4.1 and 1.1). As expected, selenite and red Se^0 were positively identified as principal components (*NSS* values 4.7 10^{-3} and 2.9 10^{-4}, respectively). Several organoselenium species including RSeR, RSeSeR, and RSSeSR were also correctly reconstructed (*NSS* values 1.2 10^{-4} to 4.3 10^{-4}). Among these five compounds retained, the most likely triplet of primary components should provide the best simulation of the whole set of bacterial spectra by linear combinations of these three spectra. Thus, all possible triplets were tested, and selenite, red Se^0 and RSeR provided the best results. Fits using RSeSeR, or RSSeSR instead of RSeR were poorer, as shown by an increase of the residual by 27%, 34% and 47%, respectively. The fact that these species were correctly reconstructed by PCA is due to their intermediate position betweeen Se^0 and RSeR (Fig. 1). The occurrence of selenocysteine (RSeH) was not tested since this compound re-oxidized to selenocystine during the experiment. However, preliminary results obtained by high performance liquid chromatography (HPLC) support the predominance of the RSeR form (L. Avoscan, R. Collins, G. Sarret, M. Carrière, J. Covès and B. Gouget (2004) Abstr. 227th ACS National Meeting, Anaheim, USA, 2004). In conclusion, alkyl selenide is believed to be the dominant organic form of Se in the bacteria exposed to selenite.

Figure 2 shows the evolution in the concentration of Se species in the bacteria during growth. Immediately after the introduction of selenite, Se was distributed as 60% Se^{IV} and 40% RSeR in the bacteria. This latter species is likely to be a reaction product of selenite rather than constitutive selenium contained in amino-acids and/or proteins since control bacteria, not exposed to selenite, did not yield a detectable Se XANES signal. Subsequently, until the end of the lag phase (t = 1h to 48h), a mixture of RSeR and Se^0 in equivalent proportions was observed. The concentration of RSeR was almost stable from 48 to 96h (18 and 15 mg Se g^{-1} of proteins, resp.), whereas the Se^0 concentration strongly increased (20 and 140 mg Se g^{-1} of proteins, resp.). At 120 and 144h, Se^0 was the only species detected. The amount of organoselenium species identified at 96h might still be present in these two samples, but masked by the dominant Se^0 form (estimated error bar : ± 5 % of total Se, *i.e.*, 13 mg g^{-1} at 120h and 17 mg g^{-1} at 144h).

In parallel experiments, selenite was added at approximately mid-exponential phase (A_{600} = 1) and at the beginning of the stationary phase (A_{600} = 3). Similar evolutions of Se accumulation and speciation were observed: Se uptake was limited for several hours, and then increased. RSeR and Se^0 were observed during the slow uptake period, followed by Se^0 only (Fig. 3). However, the production of Se^0 was faster at higher A_{600} values. For instance, after 48h exposure the bacteria contained 99.4 mg g^{-1} Se^0 compared to 19.8 mg g^{-1} Se^0 when selenite was added at an A_{600} of 1 and 0.3, respectively.

Selenate exposure

In this experiment, the bacteria were exposed to 2 mM selenate at the beginning of the growth (A_{600} = 0.3) (Fig. 4). The highest accumulation also occurred during the exponential phase, but this oxyanion was much less accumulated than selenite (the maximum concentration is 14 compared to 340 mg of Se g^{-1} of proteins for selenite). In contrast with the selenite experiment, the presence of selenate did not increase the lag phase duration. During the exponential phase, bacteria in selenate-complemented media grew at rates comparable to those of bacteria grown in selenite-free media, and maximal densities were very similar whether or not selenate was present in the culture medium (Fig. 4). The experiment was stopped after 72h since the bacterial population started to decrease, probably due to the depletion of nutrients in the medium (the same decrease was observed for the control culture). This was indicated by the decrease of absorbance, and verified by the numeration of cells forming colonies on LB agar (data not shown).

XANES spectra for the bacteria at various selenate exposure times are shown in Figure 5. The PCA of this set of spectra showed that three Se species were present (eigenvalues 73, 4.9 and 1.9): Se^{VI}, Se^{IV} and organoselenium (*NSS* values 3.7 10^{-3}, 3.3 10^{-3} and 2.7 10^{-4} to 6.6 10^{-4}, respectively). Se^0 could not be considered as a principal component (*NSS* value 1.2 10^{-2}). Using the same procedure as for the selenite experiment, we found that RSeR was the most likely organoselenium species. Se^{VI} was detected in the bacterial pellets immediately after its introduction to the culture medium (t = 0h) and at t = 12h (Fig. 5). At t = 12h, the bacteria contained Se^{IV}, Se^{VI} and RSeR. The simulation of the spectrum for t = 24h was significantly improved by adding Se^0 to the simulation (NSS value decreased by 27%), although this species was not a principal component of the system. The occurrence of only 8% Se^0 in one particular sample explains why it was not detected as principal component of the system. At longer exposure times, RSeR was the only species detected.

In another experiment, selenate was added at mid-exponential phase (A_{600} = 1). The same evolution in the speciation of selenium was observed, although Se^0 was more represented (up to 27% of total Se, Fig. 5). The slight shift of the main peak for the spectrum at t = 6h compared to t = 168h is indicative of this higher Se^0 content (Fig. 5).

The composition of headspace gas was not investigated during the selenite and selenate experiments, but the formation of volatile methylated Se species is believed to be limited since > 90% of the Se initially in solution could be accounted for upon ICP-MS analyses of the bacterial samples and solutions.

Two-contaminant (Se^{IV} and Se^{VI}) exposure

As selenite is completely reduced to Se^0, whereas selenate is not, although some selenite is produced, we have checked the hypothesis of the inhibition of the selenite reduction to Se^0 by selenate. The bacteria were thus exposed to both selenite and selenate introduced at the same time, or to one of these species first with the addition of the second one three hours later. The day after exposure, the characteristic red color of Se^0 was observed in the three experiments, both at equivalent selenite and selenate concentrations (2 mM) and with a 10-fold excess in selenate (1 mM selenite and 10 mM selenate) regardless the order of introduction. Thus, the possible inhibition of selenite reduction by selenate could be ruled out.

Discussion

The fast selenite uptake following several hours of slow uptake cannot be ascribed to the high metabolism of the cells during the exponential phase since the same profiles were observed when this oxyanion was added during the lag phase, the exponential phase or at the beginning of the stationary phase. This behavior might suggest the slow activation of some selenite transport system. To our knowledge, no specific selenite transporter has been characterized in microorganisms. In *E. coli*, selenite can enter the cell through the sulfate transporter, but the repression of this carrier does not inhibit selenite uptake completely (28). In *R. sphaeroides*, a polyol transporter is suggested as the transporting agent of selenite into the cytoplasm (4).

Could the organoselenium species observed during the period of slow uptake be an intermediate product of the formation of elemental selenium ? For *E. coli*, selenite reduction can follow a non-enzymatic pathway involving glutathione (GSH), and organoselenium intermediates include selenodiglutathione (RSSeSR) and glutathioselenol (RSSeH) (28). The fact that RSSeSR was not detected as transient species does not necessarily imply that this

non-enzymatic reduction pathway does not exist in *R. metallidurans* CH34 (the occurrence of glutathioselenol was not tested since this compound was absent from our model compounds library). The non-enzymatic reduction of selenite is accompanied by the production of $O_2^{\cdot -}$ (14), and generates an oxidative stress. In the case of *R. metallidurans* CH34, the overexpression of an enzyme associated with oxidative stress, an iron-containing superoxide dismutase, has been recently observed in the presence of selenite (23). This might support the hypothesis that non-enzymatic reduction takes place in these bacteria. Alternatively, the RSeR species observed after selenite introduction might result from an assimilatory pathway. Such a pathway is thought to exist in bacteria since Se is a composite of some bacterial enzymes such as formate dehydrogenase (27). The most commonly (non volatile) alkyl selenide species found in microorganisms is selenomethionine (6). HPLC analyses are under way to determine the exact nature of the RSeR species present in *R. metallidurans* CH34. To summarize, the presence of RSeR and Se^0 species in equivalent amounts during the period of slow uptake suggests that selenite is accumulated through two competing pathways, an assimilatory pathway and a slow detoxification pathway, with both having similar kinetics.

During the period of fast selenite uptake, the reduction pathway becomes predominant. These contrasting behaviors between the period of slow and fast uptake mirror what has been previously observed for *R. sphaeroides* at low and high selenite exposure: this bacterium metabolized selenite into approximately 60% RSeR and 40% Se^0 after exposure to 1.6 mg l^{-1} of selenite, and produced almost 100% Se^0 after exposure to 160 mg l^{-1} selenite (29). For some bacteria, selenite reduction is mediated by a single enzyme: a periplasmic nitrite reductase (16) in *Thauera selenatis*, and a nitrite or a nitrate reductase in *Enterobacter cloacae* (9, 15). The proteome analysis of *R. sphaeroides* exposed to selenite did not reveal the overexpression of a single enzyme capable of reducing selenite, but did confirm the presence of some chaperones, an elongation factor and some enzymes associated with oxidative stress (4). Garbisu *et al.* (11) showed that selenite reduction by *Bacillus subtilis* was not affected by an excess of nitrate, nitrite, sulfate or sulfite in the medium, and suggested that selenite was reduced by an inducible detoxification system different from N- and S-related reductases. The kinetics of selenite accumulation and transformation by *R. metallidurans* CH34 suggest the induction of some selenite uptake and reduction systems, whose nature remains unknown. The putative induction of selenite transport and reduction, which takes several hours, can be qualified as slow compared to the induction of the *mer* operon by Hg^{2+}, which takes a few seconds (3).

The uptake of selenate by *R. metallidurans* CH34 was strongly limited, and the bacterial growth was not affected by this oxyanion. This behavior is consistent with the general idea that selenate is slowly transported inside the cells via the sulfate permease system (13). Selenite was detected during the first 12h after selenate introduction. Several types of enzymes have been shown to reduce selenate to selenite. In *T. selenatis*, this is done by a specific selenate reductase (16, 26). In *E. coli*, reduction is catalized by a molybdenum enzyme distinct from a nitrate reductase (5). Evidence for the role of a molybdo-enzyme in selenate reduction was also shown for *Enterobacter cloacae* (31). *In vitro* studies showed that several nitrate reductases (NR) including some membrane-bound NR of *E. coli* (1) and some membrane-bound and periplasmic NR of *R. sphaeroides*, *Paracoccus denitrificans*, *Paracoccus pantotrophus* and *Ralstonia eutropha* DSM 428 (25) were able to reduce selenate under anaerobic conditions. Selenate might also be reduced by the enzymes of the sulfate assimilation pathway. Such process is known to occur in higher plants (22), but there is no direct evidence for the role of sulfate-reducing enzymes in bacterial selenate reduction. For the moment, we have no indication of the selenate reducing agent in *R. metallidurans* CH34. The occurrence of selenite is followed by a mixture of Se^0 and RSeR, and then by RSeR only. The absence of Se^0 at t = 72h can be explained by the high RSeR content which may mask Se^0 (see the error bar in Fig. 4).

In summary, our results show that selenate is partly reduced to Se^0, but that the main process is the transformation and accumulation of an RSeR-like organoselenium compound. A similar fate for selenate was observed in *R. sphaeroides*, at both low and high selenate concentrations (29). De Souza et al. (8) found that selenate-treated *Halomonas* bacteria accumulate selenate and a minor selenomethionine-like species, and suggested that selenate followed the sulfate assimilation pathway.

These results raise the question of why selenite and selenate follow different pathways, provided that selenate is first reduced to selenite. This study shows that reduction and assimilation pathways are taken by both oxyanions, and that the former pathway seems to be activated upon selenite exposure only. The possible inhibition of the reduction of selenite to Se^0 by selenate can be ruled out since the bacteria exposed to both oxyanions still produced the red color indicative of Se^0. The non-activation of the reduction pathway upon selenate exposure could be related to the much smaller uptake of selenate relative to selenite, supposing that this pathway is activated above a threshold concentration of selenite or any chemical agent derived from selenite. In this study, maximum measured selenite concentrations were comparable upon selenite and selenate exposure (around 3 mg Se per g of

proteins, Fig. 2 and 4), but these values are only snapshot images, rather than a direct monitoring of the selenite content.

In conclusion, this study showed that both selenite and selenate follow an assimilatory and a detoxification pathway in *R. metallidurans* CH34, and that transport and reduction are activated upon selenite exposure. The capacity of this bacterium to accumulate and reduce high amounts of selenite may qualify this strain as suitable for the bioremediation of selenite-contaminated soils, sediments and waters. However, the same is not true for selenate, since organoselenium species produced may represent some mobile and bioavailable forms of selenium. This study illustrates the potential of XANES spectroscopy combined with elemental analyses, which enable the quantification of Se species. This spectroscopic approach is complementary to analytical speciation techniques such as liquid or ionic chromatography, or electrospray mass spectrometry (6), which are better suited to identify individual molecules.

Acknowledgements

We acknowledge J. L. Hazemann and O. Proux for assistance during XANES measurements, and the ESRF for the provision of beamtime. This research was supported by the CNRS and CEA through the "Programme National Toxicologie Nucléaire Environnementale".

References

1. **Avazéri, C., R. Turner, J. Pommier, J. Weiner, G. Giordano, and A. Verméglio.** 1997. Tellurite reductase activity of nitrate reductase is responsible for the basal resistance of *Escherichia coli* to tellurite. Microbiology **143:**1181-1189.
2. **Avoscan, L., M. Carrière, F. Jehanneuf, R. Collins, F. Carrot, J. Covès, and B. Gouget.** 2004. *Ralstonia metallidurans* CH34 resistance to selenium oxyanions: Growth kinetics, bioaccumulation and reduction, p. 267-271. *In* J. A. Centeno, Ph. Collery, and G. Vernet (ed.), Metal Ions in Biology and Medicine, (vol. 8). John Libbey Eurotext, Montrouge, France.
3. **Barkay, T., S. Miller, and A. Summers.** 2003. Bacterial mercury resistance from atoms to ecosystems. FEMS Microbiol. Rev. **27:**355-384.
4. **Bébien, M., J. P. Chauvin, J. M. Adriano, S. Grosse, and A. Verméglio.** 2001. Effect of selenite on growth and protein synthesis in the phototrophic bacterium *Rhodobacter sphaeroides*. Appl. Environ. Microbiol. **67:**4440-4447.
5. **Bébien, M., J. Kirsch, V. Méjean, and A. Verméglio.** 2002. Involvement of a putative molybdenum enzyme in the reduction of selenate by *Escherichia coli*. Microbiology **148:**3865-3872.
6. **Chasteen, T., and R. Bentley.** 2003. Biomethylation of selenium and tellurium: Microorganisms and Plants. Chem. Rev. **103:**1-26.
7. **Combs, G. F., Jr., C. Garbisu, B. C. Yee, A. Yee, D. E. Carlson, N. R. Smith, A. C. Magyarosy, T. Leighton, and B. B. Buchanan.** 1996. Bioavailability of selenium accumulated by selenite-reducing bacteria. Biol. Trace Elem. Res. **52:**209-25.
8. **de Souza, M. P., A. Amini, M. A. Dojka, I. J. Pickering, S. C. Dawson, N. R. Pace, and N. Terry.** 2001. Identification and characterization of bacteria in a selenium-contaminated hypersaline evaporation pond. Appl. Environ. Microbiol. **67:**3785-3794.
9. **Dungan, R. S., and W. T. Frankenberger.** 1998. Reduction of selenite to elemental selenium by *Enterobacter cloacae* SLD1a-1. J. Environ. Qual. **27:**1301-1306.
10. **Ganther, H.** 1968. Selenotrisulfides. Formation by the reaction of thiols with selenious acid. Biochemistry **7:**2898-2905.
11. **Garbisu, C., S. Gonzalez, W. H. Yang, B. C. Yee, D. L. Carlson, A. Yee, N. R. Smith, R. Otero, B. B. Buchanan, and T. Leighton.** 1995. Physiological mechanisms regulating the conversion of selenite to elemental selenium by *Bacillus subtilis*. Biofactors **5:**29-37.

12. **Haygarth, P.** 1994. Global Importance and Global Cycling of Selenium, p. 1-27. *In* J. Frankenberger W.T. and S. Benson (ed.), Selenium in the Environment. Marcel Dekker, NY.

13. **Heider, J., and A. Böck.** 1993. Selenium metabolism in Micro-organisms. Adv. Microb. Physiol. **35:**71-109.

14. **Kramer, G., and B. Ames.** 1988. Mechanisms of mutagenicity and toxicity of sodium selenite (Na_2SeO_3) in *Salmonella typhimurium*. Mutat. Res. **201:**169–180.

15. **Losi, M. E., and W. T. Frankenberger.** 1998. Reduction of selenium oxyanions by *Enterobacter cloacae* strain SLDIa-I, p. 515-544. *In* W. T. Frankenberger and R. A. Engberg (ed.), Environmental Chemistry of Selenium, vol. 64. Marcel Dekker, NY.

16. **Macy, J. M.** 1994. Biochemistry of selenium metabolism by *Thauera selenatis* gen. nov. sp. nov. and use of the organism for bioremediation of selenium oxyanions in San Joaquin Valley drainage water, p. 421–444. *In* J. Frankenberger W.T. and S. Benson (ed.), Selenium in the Environment. Marcel Dekker, NY.

17. **Manceau, A., M. A. Marcus, and N. Tamura.** 2002. Quantitative speciation of heavy metals in soils and sediments by synchrotron X-ray techniques, p. 341-428. *In* P. Fenter, M. Rivers, N. Sturchio, and S. Sutton (ed.), Applications of Synchrotron Radiation in Low-Temperature Geochemistry and Environmental Science, vol. 49. Reviews in Mineralogy and Geochemistry, Mineralogical Society of America, Washington, DC.

18. **Mergeay, M., S. Monchy, T. Vallaeys, V. Auquier, A. Benotmane, P. Bertin, S. Taghavi, J. Dunn, D. van der Lelie, and R. Wattiez.** 2003. *Ralstonia metallidurans*, a bacterium specifically adapted to toxic metals: towards a catalogue of metal-responsive genes. FEMS Microbiol. Rev. **27:**385-410.

19. **Mergeay, M., D. Nies, H. G. Schlegel, J. Gerits, P. Charles, and F. Van Gijsegem.** 1985. *Alcaligenes eutrophus* CH34 is a facultative chemolithotroph with plasmid-bound resistance to heavy metals. J. Bacteriol. **162:**328-334.

20. **Pickering, I., G. George, V. Van Fleet-Stalder, T. Chasteen, and R. Prince.** 1999. X-ray absorption spectroscopy of selenium-containing amino acids. J. Biol. Inorg. Chem. **4:**791-79.

21. **Pickering, I. J., G. E. Brown, and T. K. Tokunaga.** 1995. Quantitative speciation of selenium in soils using X-ray absorption spectroscopy. Environ. Sci. Technol. **29:**2456-2459.

22. **Pilon-Smits, E. A. H., S. B. Hwang, C. M. Lytle, Y. L. Zhu, J. C. Tai, R. C. Bravo, Y. C. Chen, T. Leustek, and N. Terry.** 1999. Overexpression of ATP sulfurylase in Indian mustard leads to increased selenate uptake, reduction, and tolerance. Plant Physiol. **119:**123-132.

23. **Roux, M., and J. Covès.** 2002. The iron-containing superoxide dismutase of *Ralstonia metallidurans* CH34. FEMS Microbiol. Lett. **210:**129-133.

24. **Roux, M., G. Sarret, I. Pignot-Paintrand, M. Fontecave, and J. Covès.** 2001. Mobilization of selenite by *Ralstonia metallidurans* CH34. Appl. Environ. Microbiol. **67:**769-773.

25. **Sabaty, M., C. Avazeri, D. Pignol, and A. Vermeglio.** 2001. Characterization of the reduction of selenate and tellurite by nitrate reductases. Appl. Environ. Microbiol. **67:**5122-5126.

26. **Schröder, I., S. Rech, T. Krafft, and J. M. Macy.** 1997. Purification and characterization of the selenate reductase from *Thauera selenatis*. J. Biol. Chem. **272:**23765-23768.

27. **Stadtman, T.** 1996. Selenocysteine. Annu. Rev. Biochem. **65:**83-100.

28. **Turner, R. J., J. H. Weiner, and D. E. Taylor.** 1998. Selenium metabolism in *Escherichia coli*. Biometals **11:**223-227.

29. **Van Fleet Stalder, V., T. Chasteen, I. Pickering, G. George, and R. Prince.** 2000. Fate of selenate and selenite metabolized by *Rhodobacter sphaeroides*. Appl. Environ. Microbiol. **66:**4849-4853.

30. **Wasserman, S. R., P. G. Allen, D. K. Shuh, J. J. Bucher, and N. M. Edelstein.** 1999. EXAFS and principal component analysis: a new shell game. J. Synchr. Rad. **6:**284-286.

31. **Watts, C., H. Ridley, K. Condie, J. Leaver, D. Richardson, and C. Butler.** 2003. Selenate reduction by *Enterobacter cloacae* SLD1a-1 is catalysed by a molybdenum-dependent membrane-bound enzyme that is distinct from a membrane-bound nitrate reductase. FEMS Microbiol. Lett. **228:**273-279.

Figure captions

FIG. 1: XANES spectra for some reference compounds (in solid state unless specified). From top to bottom: sodium selenate, sodium selenite, selenourea, S-methyl seleno L-cysteine, seleno-DL cystine, selenodiglutathione (in solution), red and gray elemental selenium. The position of the maximum of the white line is indicated in parentheses.

FIG. 2: Concentration of Se species in *R. metallidurans* CH34 exposed to selenite as determined by XANES linear combination fitting and ICP-MS analyses, and time course of growth for the bacteria exposed to selenite (open circles). Error bars correspond to ± 5% of total Se.

FIG. 3: Selected Se K-edge XANES spectra for *R. metallidurans* CH34 at various incubation times after introduction of selenite into the culture medium at an A_{600} of 0.3, 1 and 3, and the distribution of Se species determined by linear combination fitting.

FIG. 4: Concentration of Se species in *R. metallidurans* CH34 exposed to selenate as determined by XANES linear combination fitting and ICP-MS analyses, and time course of growth for the bacteria exposed to selenate (open circles) and for the control culture in absence of added selenium oxyanion (filled circles). Error bars correspond to ± 5% of total Se.

FIG. 5: Selected Se K-edge XANES spectra for *R. metallidurans* CH34 at various incubation times after introduction of selenate into the culture medium at an A_{600} of 0.3 and 1, and the distribution of Se species determined by linear combination fitting.

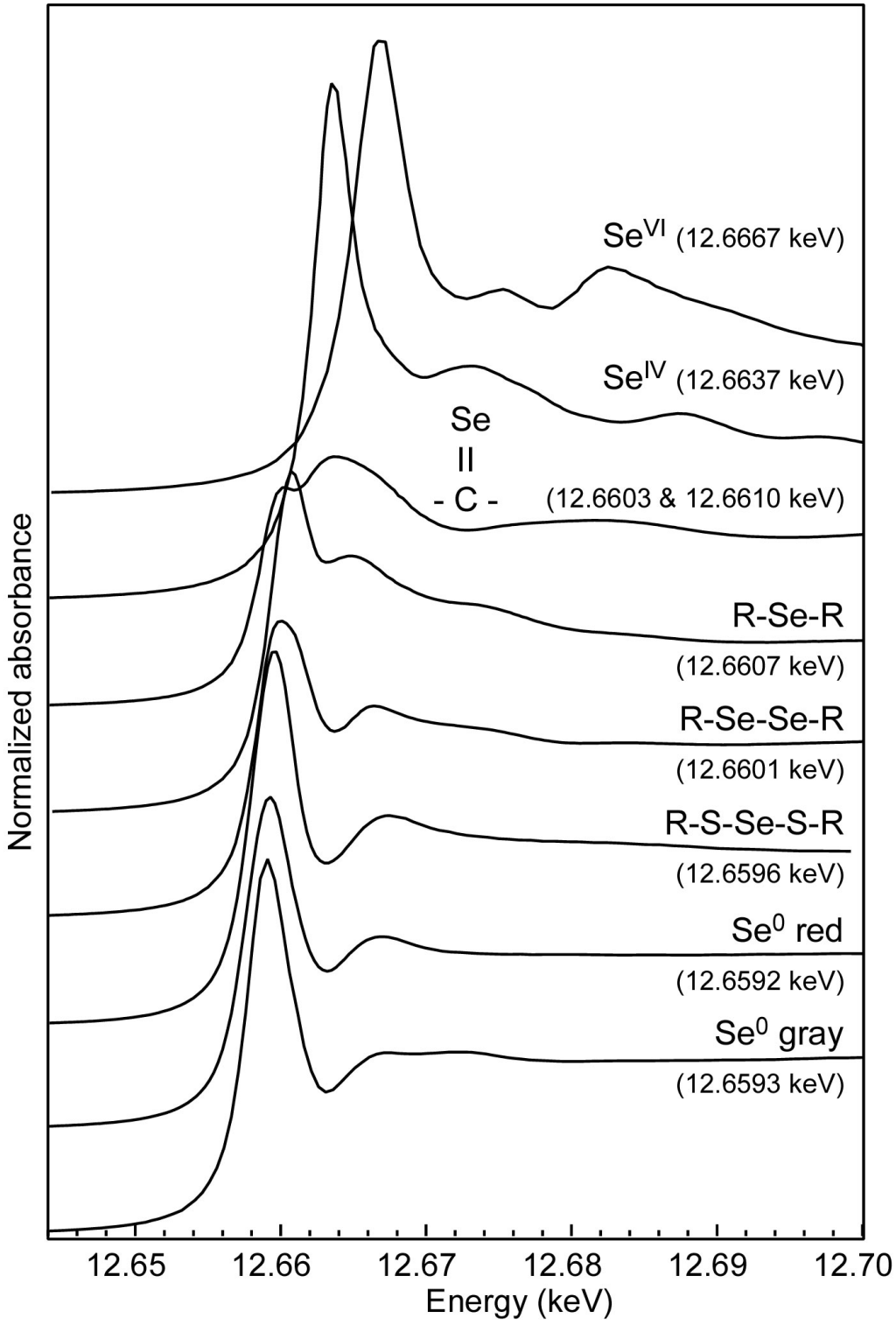
Normalized absorbance
Energy (keV)
12.65
12.66
12.67
12.68
12.69
12.70
Se^VI (12.6667 keV)
Se^IV (12.6637 keV)
Se
II
- C -
(12.6603 & 12.6610 keV)
R-Se-R
(12.6607 keV)
R-Se-Se-R
(12.6601 keV)
R-S-Se-S-R
(12.6596 keV)
Se^0 red
(12.6592 keV)
Se^0 gray
(12.6593 keV)

fig. 1

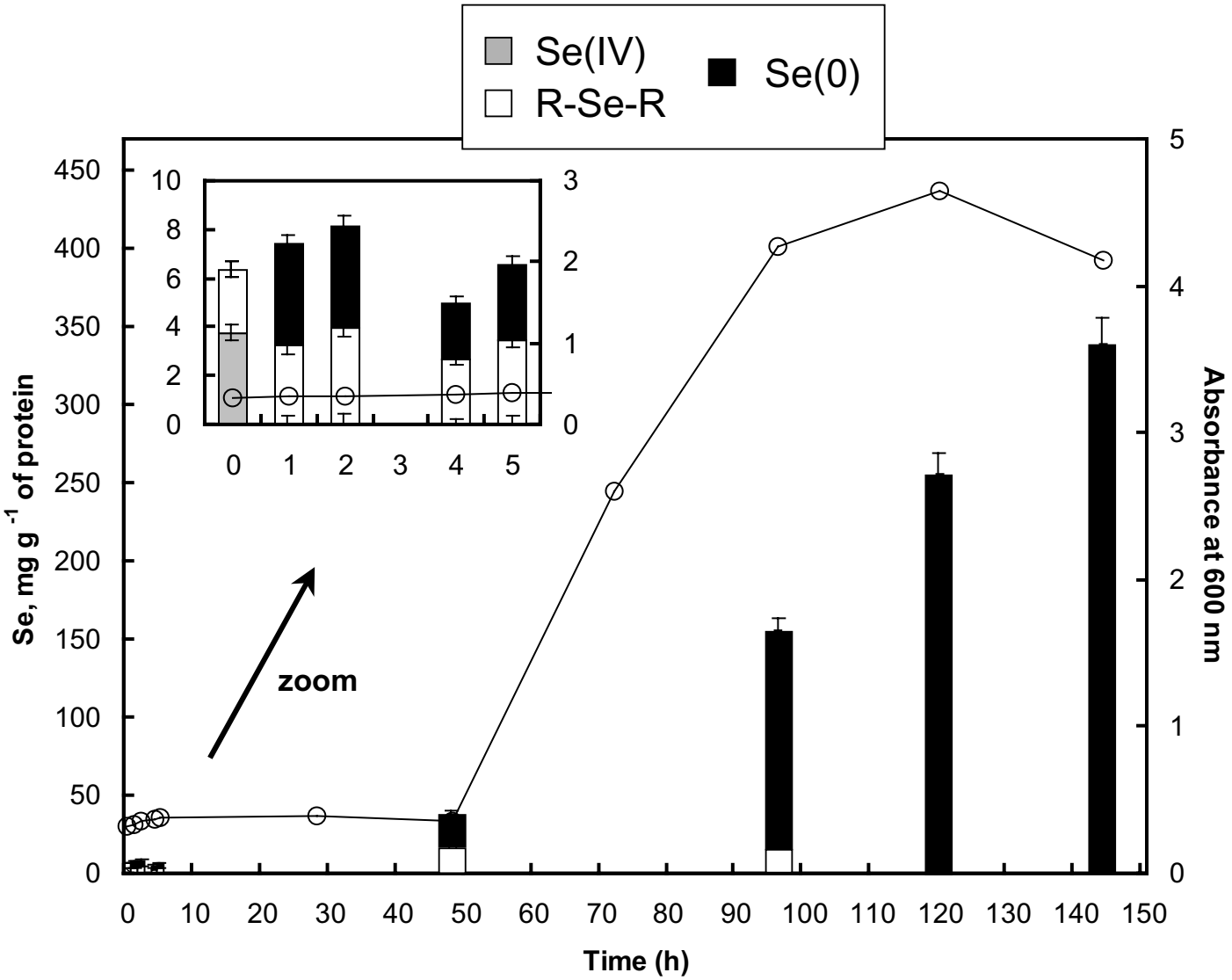
Se(IV)
R-Se-R
Se(0)
Se, mg g -1 of protein
Absorbance at 600 nm
Time (h)
zoom
0
50
100
150
200
250
300
350
400
450
0
1
2
3
4
5
0
10
20
30
40
50
60
70
80
90
100
110
120
130
140
150
0
2
4
6
8
10
0
1
2
3
4
5

fig. 2

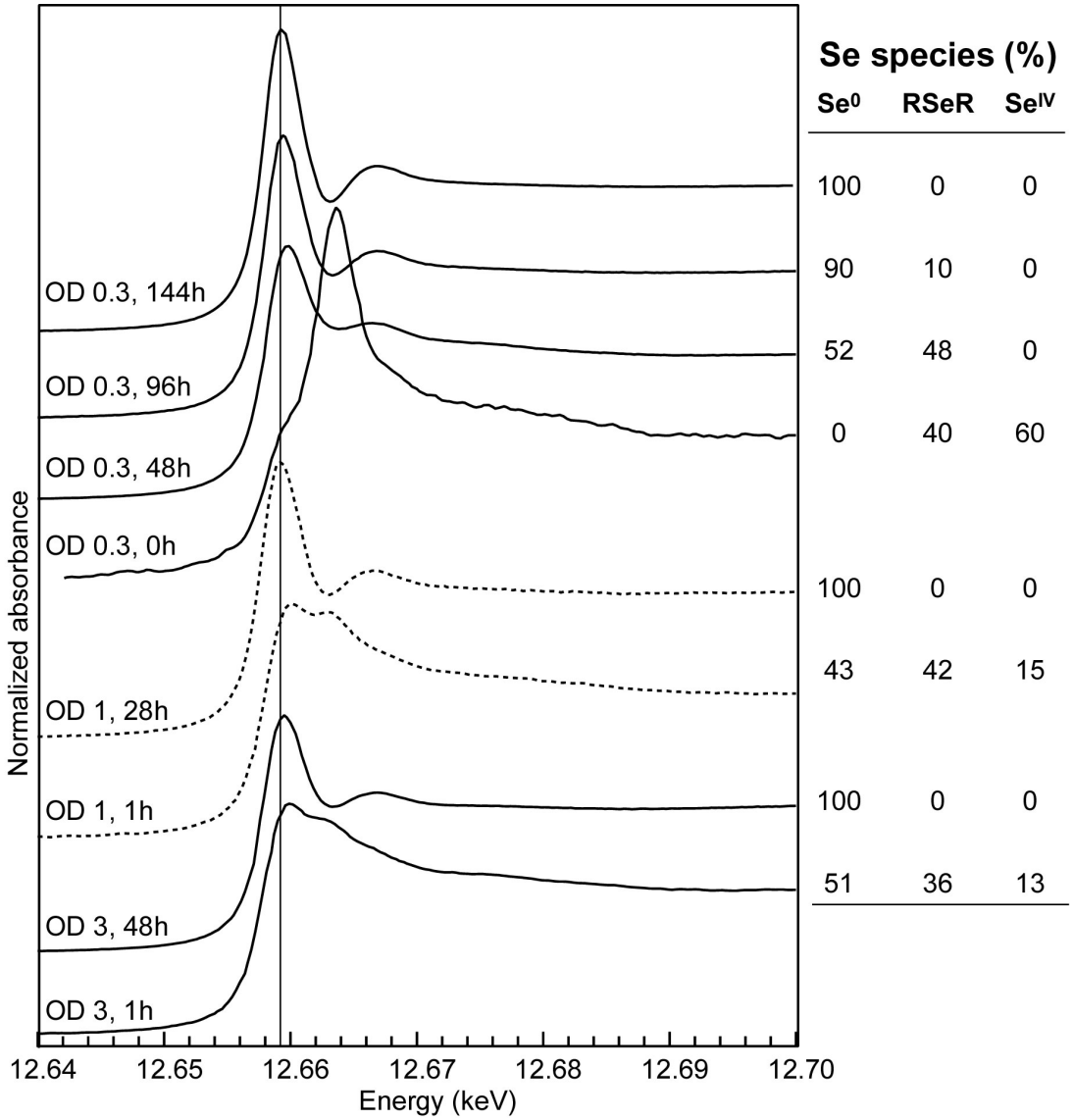

Se species (%)		
Se^0	RSeR	Se^{IV}
100	0	0
90	10	0
52	48	0
0	40	60
100	0	0
43	42	15
100	0	0
51	36	13

fig. 3

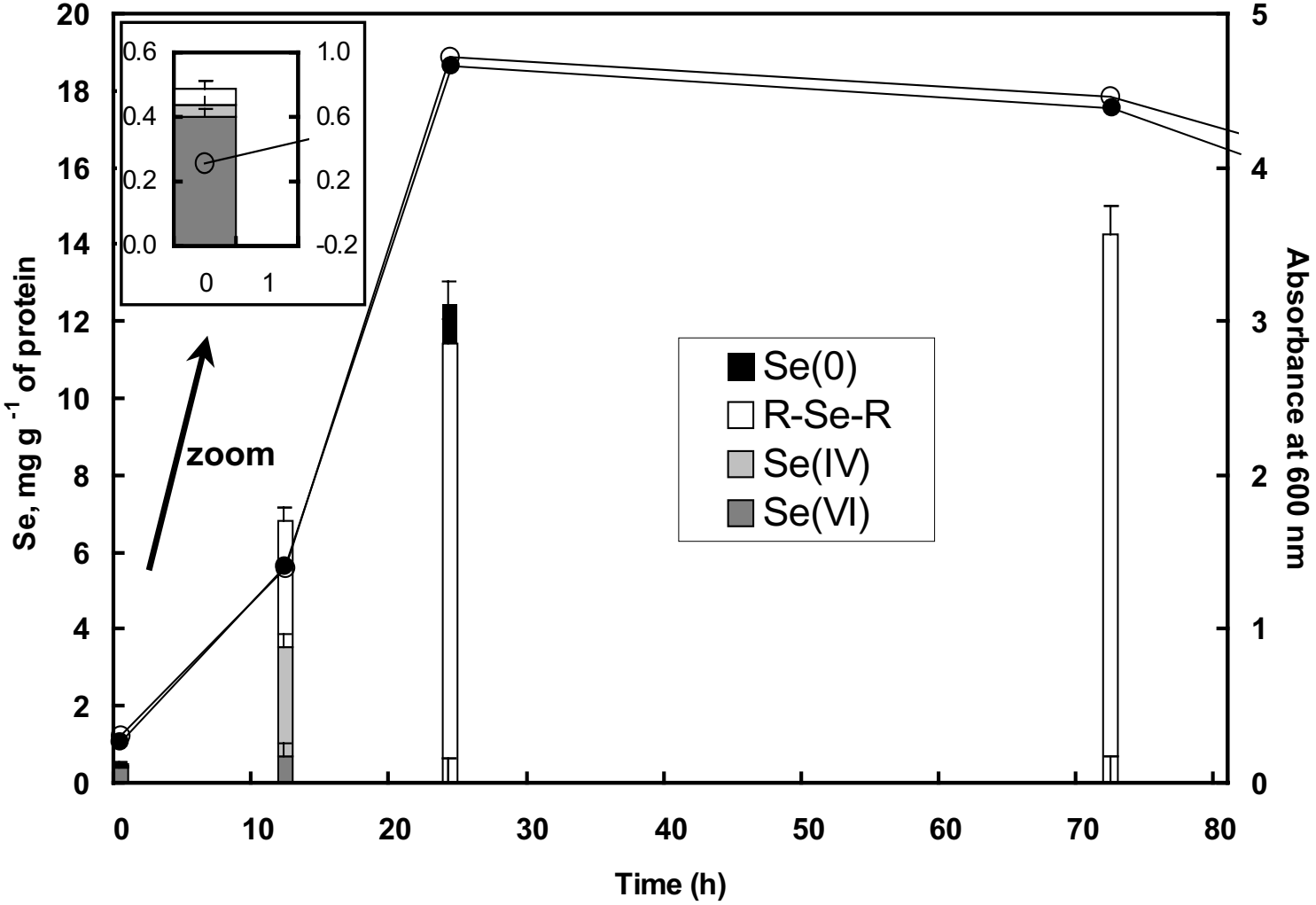
Se, mg g -1 of protein
Absorbance at 600 nm
Time (h)
zoom
Se(0)
R-Se-R
Se(IV)
Se(VI)
0
10
20
30
40
50
60
70
80
0
2
4
6
8
10
12
14
16
18
20
0
1
2
3
4
5
0.0
0.2
0.4
0.6
-0.2
0.2
0.6
1.0
0
1

fig. 4

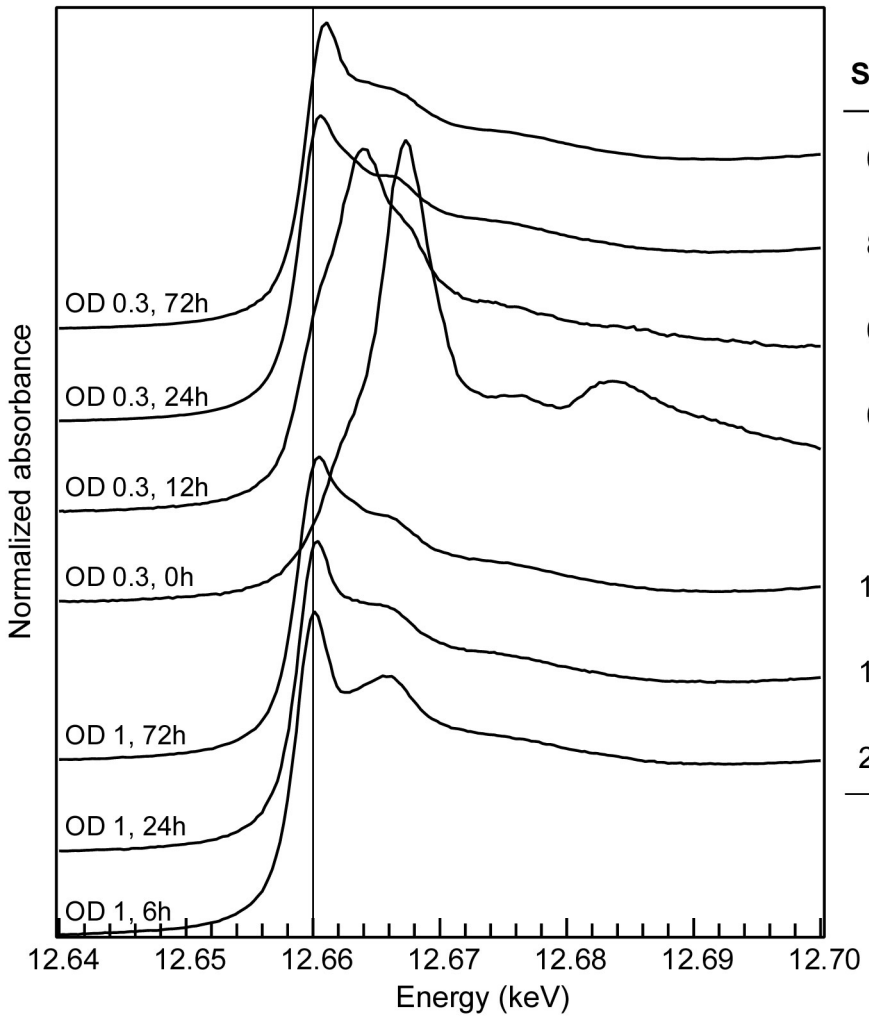

Se species (%)

Se^0	RSeR	Se^{IV}	Se^{VI}
0	100	0	0
8	92	0	0
0	48	42	10
0	11	8	81
15	85	0	0
18	82	0	0
27	70	4	0

fig. 5